Original Research Paper

Volume - 16 | Issue - 04 | April - 2026 | PRINT ISSN No. 2249 - 555X | DOI : 10.36106/ijar

Physics

GROWTH OPTIMIZATION AND CRYSTALLOGRAPHIC INVESTIGATION OF MSE_2 SINGLE CRYSTALS

Rajiv D. Vaidya — Sheth P.T. Arts & Science College, Godhra, Gujarat, India

Mehul S. Dave — Natubhai V. Patel College of Pure and Applied Sciences, Vallabh Vidyanagar, Gujarat

Kaushik. R. Patel* — Department of Microbiology, Gujarat Vidyapith, Ahmedabad, Gujarat *Corresponding Author

ABSTRACT High-quality single crystals of layered transition metal diselenides MSe_2 (M = Nb, Mo, Ta, or W) were successfully grown using the chemical vapour transport technique under optimized temperature gradients. A comparative investigation was carried out to evaluate the influence of the transition metal species on growth behaviour, crystallographic parameters, and structural quality. The growth temperature required decreases systematically from $NbSe_2$ (1173 K) to WSe_2 (1098 K), indicating a transition-metal-dependent transport kinetics. Significant variation in crystal dimension was observed, with $TaSe_2$ exhibiting the largest crystal size (84 mm^3), whereas WSe_2 showed comparatively smaller growth volume. X-ray diffraction confirmed the formation of well-defined layered hexagonal structures with lattice parameters closely matching reported values. Systematic variations in lattice constants (a and c), unit cell volume, and X-ray density were observed due to differences in atomic radius and atomic mass of the transition metals. Crystallite size estimated from peak broadening revealed superior crystallinity for $NbSe_2$ and WSe_2 compared to $MoSe_2$ and $TaSe_2$. The study demonstrates that the nature of the transition metal significantly governs crystal growth conditions, structural parameters, and crystalline quality in MSe_2 compounds.

KEYWORDS : Crystal Growth, Transition Metal, Semiconductor

INTRODUCTION

Layered transition-metal dichalcogenides (TMDCs) have attracted significant research interest owing to their remarkable structural anisotropy and tunable electronic properties. Among them, MSe_2 (M = Nb, Mo, Ta, and W) compounds exhibit diverse physical characteristics, ranging from semiconducting to metallic behavior, making them promising materials for electronic, optoelectronic, and energy-related applications (Chhowalla et al., 2013; Wang et al., 2012). Their structure consists of covalently bonded Se–M–Se layers held together by weak van der Waals forces, enabling the growth of high-quality single crystals and facilitating fundamental studies of structure–property relationships (Wilson & Yoffe, 1969).

The physical properties of TMDCs strongly depend on their crystalline quality, stoichiometry, and defect concentration. Therefore, controlled growth of bulk single crystals is crucial for reliable structural and transport investigations (Manzeli et al., 2017). Techniques such as chemical vapor transport and melt growth have been widely employed to obtain phase-pure crystals with well-defined morphologies and lattice parameters (Friend & Yoffe, 1987). Optimization of growth parameters, including the temperature gradient, transport agent concentration, and reaction duration, plays a decisive role in minimizing structural imperfections and compositional deviations.

Crystallographic characterization through X-ray diffraction (XRD) provides essential insights into phase formation, lattice constants, and structural symmetry, while compositional analyses ensure stoichiometric integrity. High-quality $NbSe_2$, $MoSe_2$, $TaSe_2$, and WSe_2 single crystals are particularly important because of their layered hexagonal structures and technologically relevant electronic features (Xi et al., 2015). In this context, systematic growth optimization combined with crystallographic investigation is necessary to establish reliable synthesis protocols and provide a structural foundation for subsequent electronic property studies.

Experimental

The furnace is the most important part of the present research work for growing crystals of TMDCs. The two-zone furnace provides an appropriate temperature gradient over the entire ampoule. Typically, the temperatures employed are high. The temperature gradient within the furnace was required to be over a length of approximately 25 cm. Temperature stability plays an important role; therefore, electronic temperature controllers were used for this purpose.

High-purity fused quartz ampoules (22 mm ID, 25 mm OD, 250 mm length) were used for crystal growth, thoroughly cleaned through sequential acid treatments (HNO_3, HF, H_2SO_4), rinsed with double distilled water, heat-treated, and dried to ensure contamination-free and moisture-free conditions. Stoichiometric elemental mixtures (10 g) were loaded into the cleaned ampoules, evacuated carefully to ~10^{-5} torr to prevent material loss, flame-sealed under vacuum, and homogenized prior to the crystal growth experiments.

High-purity (99.99%) elemental precursors of Nb, Mo, Ta, W, and Se were weighed in stoichiometric proportions to prepare MSe_2 charge materials. The powdered constituents were uniformly distributed along the length of a sealed evacuated ampoule and were placed coaxially in a horizontal furnace. The temperature was gradually increased at a controlled rate of 50°C/h up to 700 °C to avoid rapid exothermic reactions and possible pressure buildup. The ampoule was maintained at 700 °C for 72 h to ensure a complete reaction and phase formation. Subsequently, slow cooling at 50°C/h yielded homogeneous, free-flowing, shiny polycrystalline MSe_2 compounds suitable for further crystal growth.

The synthesized charge was homogenized by vigorous shaking and subsequently transferred to a pre-cleaned quartz ampoule for crystal growth. Iodine (5 mg cm^{-3} of ampoule volume), sealed in thin glass capillaries, was introduced as the transport agent, and the ampoule was evacuated to ~10 °F before flame sealing. The sealed ampoule was placed in a dual-zone horizontal furnace with a controlled temperature gradient, and the temperature was raised at 20 °C h^{-1} to the desired growth conditions. The growth duration was maintained for approximately 7 days, followed by slow cooling at the same rate as room temperature. The ampoule was carefully retrieved and opened to collect well-formed single crystals.

Table 1 Growth Parameters of MSe_2 (M = Nb, Mo, Ta and W) Single Crystals.

Crystal	Temperature distribution		Growth Period (hr)	Dimension (mm^3)
	Reaction Zone (K)	Growth Zone (K)		
NbSe2	1173	1123	192	24
TaSe2	1148	1098	240	84
Mose2	1123	1073	168	28
WSe2	1098	1048	168	21

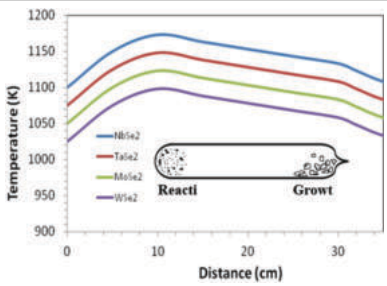

Figure 1 The Temperature Profile used for the Growth of MSe_2 Single Crystals

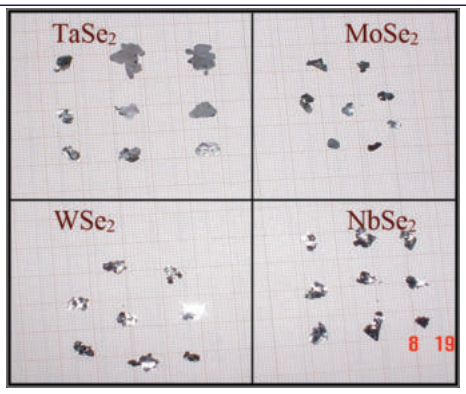

Figure 2 Photograph of MSe_2 (M = Nb, Mo, Ta, and W) as-Grown Crystals.

X-ray diffraction (XRD) is a powerful, non-destructive technique that is widely used to determine the crystal structure, lattice parameters, phase identification, crystal orientation, defects, and residual stresses in bulk and thin-film materials. Using monochromatic radiation and diffractometer systems, XRD enables precise d-spacing calculations and high-sensitivity analysis across diverse materials, including metals, ceramics, thin films, and electronic, magnetic, and biological materials. The X-ray diffractograms of $NbSe_2$, $MoSe_2$, $TaSe_2$ and WSe_2 are shown in Figures 3.

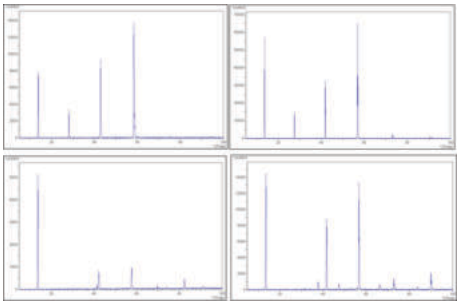

Figure 3 X-ray Diffractogram of the MSe_2 Single Crystal

RESULTS AND DISCUSSION

High-quality single crystals of MSe_2 (M = Nb, Mo, Ta, or W) were successfully grown using the chemical vapor transport technique with iodine as the transport agent. The optimized temperature distribution shows that higher reaction-zone temperatures are required for $NbSe_2$ and $TaSe_2$, while comparatively lower temperatures are sufficient for $MoSe_2$ and WSe_2. This trend indicates that heavier transition metals such as W require relatively lower transport temperatures, possibly due to differences in vapour pressure and transport efficiency of the metal iodides during CVT growth. The growth period varied from 168 to 240 hours. $TaSe_2$ required the longest growth duration (240 h), which resulted in the largest crystal dimension (84 mm^3). In contrast, WSe_2 produced smaller crystals (21 mm^3) despite similar growth duration, suggesting slower lateral growth kinetics.

The as-grown crystals exhibited a typical thin platelet morphology with smooth surfaces and metallic luster, consistent with the layered nature of transition-metal dichalcogenides. The large lateral dimensions and well-defined crystal facets indicate controlled nucleation and anisotropic growth along the basal planes driven by the van der Waals bonded layered structure.

The EDAX compositional analysis verified the near-stoichiometric proportions of the constituent elements with negligible impurity incorporation. The absence of detectable contamination demonstrates the effectiveness of optimized ampoule preparation, evacuation, and sealing procedures.

Powder X-ray diffraction patterns confirmed the formation of single-phase hexagonal structures for all compounds without detectable secondary phases. The sharp and intense diffraction peaks reflected the high crystallinity of the grown crystals. XRD patterns show dominant (00l) reflections in $NbSe_2$, $MoSe_2$, and WSe_2, indicating preferred growth along the c-axis, characteristic of layered dichalcogenides. Peak intensity analysis shows the Highest peak intensity observed in $MoSe_2$ & $NbSe_2$ and $TaSe_2$ exhibits comparatively lower intensity peaks. Higher peak sharpness and larger crystallite size confirm improved structural ordering and fewer microstrains in $NbSe_2$ and Wse_2.

The density " of the grown crystals was calculated using the following equation:

$$\rho = \frac{\sum A}{VN} \quad (1)$$

where ΣA is the total weight of the atoms in the unit cell = MZ.
M is the molecular weight and Z is the number of molecules per unit cell.
N is the Avogadro number and V is the volume of the unit cell for the hexagonal system, given by

$$\frac{\sqrt{3}}{2} a^2c \text{ Å}^3 = 0.866\, a^2c \text{ Å}^3 \quad (2)$$

The values of the lattice parameters a(Å), b(Å), c(Å), X-ray density, and unit cell volume ($Å^3$) obtained from the diffraction data for the as-grown crystals of $NbSe_2$ $MoSe_2$, $TaSe_2$ and WSe_2 are presented in Table 2 and compared with the reported data (Creazzo, F. et al. 2023). The calculated lattice parameters were in good agreement with previously reported standard values, confirming the phase purity and structural stability. The c-parameter shows significant enhancement for $TaSe_2$ (~19.22 Å), confirming its different polytype stacking compared to other compounds (~12–13 Å range). $TaSe_2$ exhibits the largest volume (196.70 $Å^3$), consistent with its large c-parameter and layered stacking nature.

Table 2 Structural Parameters of the MSe_2 (M= Nb, Mo, Ta, and W) Single Crystals.

Parameter	NbSe2	MoSe2	TaSe2	WSe2
a = b (Å)	3.490.058	3.160.009	3.440.002	3.280.012
a = b (Å) Reported	3.51	3.27	3.43	3.28
c (Å)	12.280.058	12.920.195	19.220.026	12.980.028
c (Å) Reported	12.55	12.92	19.17	12.98
Volume (Å)3	66.24	111.56	196.70	119.32
X-ray density (gm/cm3)	6.29	7.54	8.58	10.41

To determine the grain size distribution in $NbSe_2$, $MoSe_2$, $TaSe_2$ and WSe_2 single crystals, the particle size was calculated using Scherrer's formula:

$$t = \frac{k\lambda}{\beta_{2\theta}\cos\theta_0} \quad (3)$$

where t is the crystallite thickness measured perpendicular to the reflecting plane, k is Scherrer's constant whose value is chosen as unity, assuming the particles to be spherical, is the wavelength of the X-ray radiation, $_2$ is the width at half the maximum intensity measured in radians, and $_0$ is the Bragg angle. Table 3 records the crystallite sizes of the four samples.

For hexagonal close-packed structures, the growth fault probability (α) and deformation fault probability (β) can be quantitatively estimated from half-width analysis of the X-ray diffraction peaks. Reflections satisfying the condition h − k = 3n were insensitive to stacking faults, whereas reflections with h − k = 3n ± 1 and l ≠ 0 were influenced by structural faults. Therefore, the fault probabilities can be evaluated using the established analytical expressions for (hkl) reflections with even l values.

$$3\alpha + 3\beta = \frac{\beta_{2\theta} \times \pi^2 \times c^2}{360 \times l \times d^2 \times \tan\theta} \quad (4)$$

where $_2$ is the full width at half the maximum intensity expressed in degrees, c = d_{002}, l is the Miller index in the (h k l) plane for which the estimation of " and " is being made, 'd' is the inter planer spacing for (h k l) reflection in question, is the Bragg angle corresponding to this (h k l) plane.

The formula for the (h k l) values with 'l' odd is given as

$$(3\alpha + \beta) = \frac{\beta_{2\theta} \times \pi^2 \times c^2}{360 \times l \times d^2 \times \tan\theta} \quad (5)$$

From the equations 1, 2 & 3, by measuring the half width for reflections with both even and odd values of 'l' it is possible to calculate the stacking fault probabilities α & β. Instrumental broadening was neglected when calculating the half-width of the reflections. Table 4 presents the estimation results for and.

Table 3 hkl Reflections, d-spacing, 2θ Values, Peak Intensity, $_2$Values, and Particle Sizes of the MSe_2 Single Crystals.

Crystal	(h k l)	d-spacing	Angle 2θ (degree)	Peak Intensity counts/sec.	Tip Width 2θ	Particle Size (Å)
NbSe2	0 0 1	6.25	14.15	8586.48	0.12	758.62
	0 0 2	3.13	28.48	2042.24	0.12	836.91
	1 0 0	3.00	29.72	161.48	0.15	677.63
	1 0 3	1.72	53.16	377.52	0.15	981.73
	0 1 1	2.69	33.26	479.78	0.18	586.50
MoSe2	0 0 2	6.46	13.63	12596.41	0.48	185.19
	1 0 2	2.60	34.63	29.76	0.48	192.61
	1 0 3	2.37	37.81	113.94	0.36	259.16
	1 0 5	1.91	47.39	121.64	0.36	267.76
	1 0 6	1.72	56.92	37072.91	0.36	278.89
TaSe2	1 0 3	2.71	32.98	24.20	0.36	255.83
	1 1 0	1.72	53.25	32.65	0.36	274.41
	0 2 6	1.35	69.69	73.43	0.36	298.92
	2 0 5	1.40	66.49	12.65	0.72	146.66
	1 2 0	1.12	86.50	11.00	0.72	168.41
WSe2	1 0 3	2.38	37.79	288.55	0.21	444.27
	0 0 6	2.16	41.68	4347.77	0.15	630.29
	0 0 8	1.62	56.69	4647.77	0.30	343.31
	1 1 9	1.09	89.90	876.77	0.12	1039.36
	2 1 0	1.08	90.18	504.36	0.12	1041.90

Table 4 Estimation of Stacking Fault Probability of as-Grown Crystals

Crystal	(h k l)	3α + 3β	3α + β	α	β
NbSe2	1 0 3	-	0.036	0.0165	0.0135
	2 0 1	-	0.090		
	1 0 2	0.055	-		
	2 0 2	0.126	-		
MoSe2	1 0 3	-	0.285	0.065	0.047
	1 0 5	-	0.206		
	1 0 2	0.520	-		
	1 0 8	0.160	-		
TaSe2	1 0 3	-	0.559	0.347	-0.196
	2 0 5	-	1.135		
	2 0 6	0.478	-		
	2 0 8	0.429	-		
WSe2	1 0 3	-	0.167	0.026	0.039
	1 0 5	-	0.069		
	1 0 8	0.053	-		
	2 0 4	0.339	-		

Evaluation of the growth and deformation fault probabilities revealed low stacking fault density, further supporting the high structural quality of the crystals. The observed platelet growth morphology, crystallographic data, and defect analysis collectively confirm that the optimized growth conditions provide a reliable route for producing structurally superior MSe_2 single crystals that are suitable for advanced electronic and high-pressure investigations.

The comparative study clearly indicates that the transition metal influences on Transport temperature requirement, Growth kinetics and final crystal dimension, Lattice parameters and stacking nature, Unit cell volume, X-ray density, Crystallite size and structural quality. The heavier 5d metals (Ta, W) exhibit higher density and modified stacking behavior, while 4d metals (Nb, Mo) show comparatively smaller density but better crystallinity in optimized conditions.

CONCLUSION

Single crystals of MSe_2 (M = Nb, Mo, Ta, and W) were successfully grown under optimized CVT conditions, and a systematic comparative analysis was performed. The required growth temperature decreases from $NbSe_2$ to WSe_2, demonstrating a transition-metal-dependent transport mechanism. $TaSe_2$ exhibits the largest unit cell volume and crystal size due to its extended c-axis stacking, whereas WSe_2 shows the highest X-ray density owing to its larger atomic mass. XRD analysis confirms phase purity and layered hexagonal symmetry for all compounds, with lattice parameters closely matching reported values. Crystallite size estimation reveals superior crystallinity for $NbSe_2$ and WSe_2 compared to $MoSe_2$ and $TaSe_2$.

REFERENCES

1. Chhowalla, M., Shin, H. S., Eda, G., Li, L. J., Loh, K. P., & Zhang, H. (2013). The chemistry of two-dimensional layered transition metal dichalcogenide nanosheets. Nature Chemistry, 5(4), 263–275. https://doi.org/10.1038/nchem.1589
2. Creazzo, F., Jaramillo-B, L., Torres, C. M. S. (2023). Engineering of $MoSe_2$ and WSe_2 monolayers and heterostructures by molecular dynamics simulations. ACS Applied Materials & Interfaces, 15(23), 27310–27319. https://doi.org/10.1021/acsami.5c07971
3. Friend, R. H. and Yoffe, A. D. (1987). Electronic properties of intercalation complexes of transition-metal dichalcogenides. Advances in Physics, 36(1), 1–94. https://doi.org/10.1080/00018738700101951
4. Manzeli, S., Ovchinnikov, D., Pasquier, D., Yazyev, O. V., & Kis, A. (2017). 2D transition metal dichalcogenides. Nature Reviews Materials, 2, 17033. https://doi.org/10.1038/natrevmats.2017.33
5. Wang, Q. H., Kalantar.Zadeh, K., Kis, A., Coleman, J. N., & Strano, M. S. (2012). Electronics and optoelectronics of two-dimensional transition metal dichalcogenides. Nature Nanotechnology, 7(11), 699–712. https://doi.org/10.1038/nnano.2012.193
6. Wilson, J. A. & Yoffe, A. D. (1969). Transition metal dichalcogenides: Discussion and interpretation of observed optical, electrical, and structural properties. Advances in Physics, 18(73), 193–335. https://doi.org/10.1080/00018736900101307
7. Xi, X., Wang, Z., Zhao, W., Park, J. H., Law, K. T., Berger, H., Forró, L., Shan, J., & Mak, K. F. (2015). Ising pairing in superconducting $NbSe_2$ atomic layers. Nature Physics, 12, 139–143. https://doi.org/10.1038/nphys3538